Reviewer 2

The manuscript titled *"Decoding the Architecture of Drought: SHAP-Enhanced Insights into the Climate Forces Reshaping the Sahel"* presents a robust, interdisciplinary analysis of drought patterns in the Sahel region. The authors employ a multi-method approach that combines the Standardized Precipitation Evapotranspiration Index (SPEI), Seasonal Kendall (SK) trend analysis, cross-correlation with 31 climatic indices, and a SHAP-enhanced clustering methodology using Random Forest (RF) to explore the spatial-temporal variability of drought and its climatic drivers.

Key findings include:

- A significant downward trend in SPEI-12 across 57.5% of the Sahel, particularly in the west and southeast, indicating intensified drought conditions.
- Strong negative correlations between drought severity and Global Mean Temperature (GMT) and Indo-Pacific Warm Pool (IPWP); Atlantic Multidecadal Oscillation (AMO) showed spatially heterogeneous impacts.
- The clustering analysis delineates three distinct regions with unique drought dynamics and climate-drought interactions.
- The SHAP framework reveals the differential contribution of climatic indices to drought clustering, offering high interpretability and novel insight into region-specific vulnerabilities.

We sincerely thank the Reviewer for the thoughtful and thorough evaluation of our manuscript. The manuscript has been revised in accordance with all comments received. Additional modifications have also been made during the revision process, which have contributed to improving the overall quality and clarity of the text. It is hoped that the revised version will be found suitable for publication. A point-by-point response to the Reviewer's comments is provided below.

Title and Abstract

- Include quantitative results (e.g., number of clusters, correlation values) in the abstract to enhance clarity and impact.
- Slightly reduce jargon in the abstract for broader accessibility (e.g., explain "SHAP" in simpler terms before the acronym).

Thanks for the comment. The Abstract has been improved including quantitative results and slightly reducing jargon in the abstract for broader accessibility.

Introduction

- Include a short paragraph summarizing existing clustering approaches and why SHAP-RF is a significant improvement.
- Reduce the length of some paragraphs to improve readability and flow.

The Introduction has been revised by shortening several paragraphs to enhance readability and flow, and by adding a paragraph summarizing existing clustering approaches and explaining why the SHAP framework represents a significant improvement:

A critical yet frequently overlooked aspect of drought characterization involves identifying spatially homogeneous regions that exhibit consistent drought-climate relationships. Traditionally, clustering techniques such as K-means and Hierarchical clustering have been used to delineate these regions based on hydroclimatic features. K-means, while computationally efficient, assumes spherical clusters and equal variance, often oversimplifying complex spatial patterns. Hierarchical clustering, although more flexible in capturing nested relationships, can be sensitive to noise and lacks scalability for large datasets. Moreover, both methods operate as unsupervised learning algorithms, providing little insight into the underlying climatic drivers that influence cluster formation. As a result, these techniques often fall short in interpretability and in explaining the climatic processes shaping spatial drought variability.

To overcome these limitations, this study introduces an innovative SHAP-driven clustering framework, which integrates RF classification with SHAP analysis. In this approach, RF is used to classify observations into drought-prone clusters identified during the unsupervised phase, while SHAP quantifies the contribution of each climatic variable to the predicted cluster membership. This combination offers a transparent and interpretable alternative to traditional clustering by uncovering not only the spatial patterns of drought but also the relative importance of different climate drivers in shaping those patterns. The framework shifts from a purely data-partitioning paradigm to one that integrates explainable AI, significantly enhancing the understanding of how climatic variability governs regional drought dynamics.

Materials and Methods

- Consider summarizing the 31 climate indices in a supplementary table only, instead of the main text, or condensing Table 1.

  Thanks for the comment. Table 1 has been updated to include a more concise descriptions of each index, highlighting their potential impacts on Africa and the Sahel where relevant, and the data source.

Climate index	Abbr.	Definition	Data source
Atlantic Meridional Mode	AMM	The AMM describes north-south SST differences in the tropical Atlantic. Its positive phase shifts rainfall northward, increasing Sahel precipitation and reducing drought risk. The negative phase causes southward rainfall shifts,	https://psl.noaa.gov/data/timeseries/month/DS/AMM/

		leading to Sahel drought. AMM also affects Atlantic hurricane activity, influencing regional climate variability.	
Atlantic Multidecadal Oscillation	AMO	The Atlantic Multidecadal Oscillation refers to natural variations in North Atlantic Ocean sea surface temperatures that occur over periods of 20 to 40 years. In its positive phase, North Atlantic temperatures are above average, leading to hotter summers along the eastern U.S., increased hurricane activity in the tropical Atlantic, and enhanced rainfall in Africa. In its negative phase, cooler Atlantic temperatures are associated with weaker hurricane activity, drought in Africa's Sahel region, and cooler, wetter summers in Europe. The AMO plays a significant role in shaping global climate systems and regional weather patterns, particularly in the North Atlantic region.	https://www.psl.noaa.gov/data/timeseries/AMO/
Arctic Oscillation	AO	The AO influences atmospheric circulation patterns that can extend to the Sahel region by affecting the strength and position of the African Easterly Jet and mid-latitude weather systems. Its negative phase can weaken the jet stream, altering rainfall patterns in West Africa and contributing to Sahel drought or variability in seasonal precipitation.	https://psl.noaa.gov/data/timeseries/month/DS/AO/
Berkeley Earth Surface Temperature	BEST	The BEST dataset provides global and regional surface temperature trends, including detailed temperature anomalies across Africa. These trends are crucial for understanding how warming influences Sahel hydroclimate, as rising temperatures can exacerbate drought conditions and impact rainfall variability in the region.	https://psl.noaa.gov/data/correlation/censo.data
Caribbean Index	CAR	The CAR index captures climate variability in the Caribbean, including SST and atmospheric patterns. It influences Atlantic tropical cyclone activity, which can affect West African monsoon dynamics and Sahel rainfall through atmospheric teleconnections.	https://psl.noaa.gov/data/correlation/CAR_ersst.data
Eastern Pacific Oscillation Index	EPO	The EPO describes atmospheric pressure anomalies in the eastern North Pacific. Its phases influence the jet stream and temperature patterns in North America, which can indirectly affect West African climate by modulating large-scale atmospheric circulation and teleconnections linked to Sahel rainfall variability.	https://psl.noaa.gov/data/correlation/epo.data
Greenland Blocking Index	GBI	The GBI measures persistent high-pressure systems over Greenland. Its positive phase alters North Atlantic circulation, which can influence the West African monsoon and Sahel rainfall by affecting atmospheric patterns that modulate moisture transport into the region.	https://psl.noaa.gov/data/correlation/gbi.ncep.day
Global Mean Temperature	GMT	GMT tracks overall atmospheric and ocean warming or cooling trends. Rising global temperatures influence the Sahel by intensifying droughts, altering rainfall patterns, and impacting regional water resources through shifts in the hydrological cycle.	https://psl.noaa.gov/data/correlation/gmsst.data
Indo-Pacific Warm Pool	IPWP	The IPWP, with some of the warmest tropical ocean temperatures, drives global atmospheric circulation, including monsoons. Its warming phase enhances convection and rainfall, indirectly influencing Sahel rainfall through shifts in the Walker circulation and global moisture transport.	https://psl.noaa.gov/data/correlation/pacwarm.data
The North Atlantic Oscillation	NAO	The NAO index measures sea-level pressure differences between the Azores High and the Subpolar Low. Its phases modulate the North Atlantic jet stream and storm tracks, affecting heat and moisture transport. These changes influence West African monsoon strength and Sahel precipitation by altering atmospheric circulation patterns over the Atlantic.	https://psl.noaa.gov/data/correlation/nao.data
The North Atlantic Oscillation (Jones)	NAO (Jones)	Defined by Jones (1997), this NAO index measures the sea-level pressure difference between the Azores High and Icelandic Low. Its phases influence Atlantic atmospheric circulation patterns that affect West African monsoon dynamics and Sahel rainfall variability.	https://psl.noaa.gov/data/correlation/jonesnao.data
Niño-1.2	-	This index covers sea surface temperatures in the eastern equatorial Pacific (80°W–90°W, 10°S–0°), where El Niño and La Niña events typically originate. In its positive phase (El Niño), warmer waters lead to increased rainfall and floods along South America’s northwest coast; in its negative phase (La Niña), cooler waters cause drought and promote cold-water upwelling. While its direct effects are regional, Niño-1+2 influences large-scale atmospheric circulation patterns, which can alter the West African monsoon strength and consequently affect Sahel precipitation variability.	https://www.cpc.ncep.noaa.gov/data/indices/ersst5.nino.mth.91-20.ascii
Niño 3	-	The Niño-3 index tracks sea surface temperatures in the eastern equatorial Pacific (150°W–90°W, 5°S–5°N) to monitor El Niño and La Niña events.	https://www.cpc.ncep.noaa.gov/data/

		During El Niño (positive phase), warmer waters cause increased rainfall in western South America, drought in Asia-Pacific, and reduced rainfall in the Sahel. La Niña (negative phase) brings cooler waters, increased storms in Asia-Pacific, and enhanced rainfall in the Sahel. This index influences global atmospheric circulation and tropical rainfall patterns.	indices/ersst5.nino.mth.91-20.ascii
Niño-3.4	-	The Niño-3.4 index measures sea surface temperatures in the central equatorial Pacific (120°W–170°W, 5°S–5°N) and is a key indicator of El Niño and La Niña events. During El Niño (positive phase), warmer waters lead to increased rainfall along South America's coast, drought and heatwaves in the Asia-Pacific, and reduced rainfall in the Sahel. La Niña (negative phase) brings cooler waters, heavy rains and floods in Asia-Pacific, drought in South America, and enhanced rainfall in the Sahel. Niño-3.4 strongly influences global atmospheric circulation and tropical weather patterns.	https://www.cpc.ncep.noaa.gov/data/indices/ersst5.nino.mth.91-20.ascii
Niño-4	-	The Niño-4 index measures sea surface temperature variations in the central Pacific (160°E–150°W, 5°S–5°N) during El Niño and La Niña events. In its positive phase (El Niño), warmer waters enhance convection in the tropical western Pacific, influencing atmospheric circulation and monsoon patterns, often linked to reduced rainfall in the Sahel. In the negative phase (La Niña), cooler waters lead to drought in the western Pacific and increased rainfall in the central Pacific, sometimes boosting Sahel precipitation. Niño-4 is key for understanding tropical circulation and regional climate variability.	https://www.cpc.ncep.noaa.gov/data/indices/ersst5.nino.mth.91-20.ascii
Northern Oscillation Index	NOI	The NOI measures sea level pressure differences between Tahiti (eastern tropical Pacific) and Darwin (western subtropical Pacific). In its positive phase, high pressure dominates the eastern Pacific and low pressure the western Pacific, causing drought in the east and wetter conditions in the west. The negative phase reverses this pattern. The NOI is essential for understanding tropical climate phenomena such as El Niño-Southern Oscillation (ENSO) impacts.	https://psl.noaa.gov/data/correlation/noi.data
North Pasific Index	NP	The NP reflects average sea level pressure over the North Pacific, indicating the strength of the Aleutian Low. In its positive phase, a stronger Aleutian Low brings more rainfall to western North America and cooler eastern Pacific waters. In the negative phase, the system weakens, leading to drier conditions and warmer sea surface temperatures. The NP Index is key to understanding Pacific atmospheric circulation and its effects on North American and, to a lesser extent, African climate patterns	https://psl.noaa.gov/data/correlation/np.data
North Tropical Atlantic SST Index	NTA	The NTA index represents SSTs in the North Tropical Atlantic. In its positive phase, warmer SSTs enhance convection and tropical cyclone activity, while influencing rainfall patterns across the Atlantic basin. This phase is often linked to increased precipitation in the Sahel. In the negative phase, cooler SSTs reduce cyclone activity and can lead to drought conditions in West Africa. The NTA index is crucial for understanding Atlantic climate variability and its impacts on regional weather systems.	https://psl.noaa.gov/data/correlation/NTA_ersst.data
Oceanic Niño Index	ONI	The ONI measures the three-month running average of sea surface temperature anomalies in the Niño-3.4 region of the central tropical Pacific. It is the primary indicator of El Niño and La Niña events within the ENSO cycle. Positive ONI values (El Niño) are linked to drought in regions like Australia and the Sahel, while negative values (La Niña) can enhance rainfall in these areas. The ONI is essential for monitoring ENSO's global impacts on temperature, rainfall, and atmospheric circulation	https://psl.noaa.gov/data/correlation/oni.data
Pasific Decadal Oscillation	PDO	The PDO describes long-term shifts in sea surface temperatures and atmospheric pressure across the North Pacific. In its positive phase, the eastern Pacific cools while the western Pacific warms, bringing wetter conditions to western North America and warmer weather in Alaska. In the negative phase, the pattern reverses, causing drought in western North America and reduced marine productivity. The PDO influences multi-decadal climate variability, affecting agriculture, fisheries, and water resources globally, including rainfall patterns in Africa	https://psl.noaa.gov/data/correlation/pdo.data
Pacific Meridional Mode	PMM	The PMM is a climate pattern driven by interactions between sea surface temperatures and surface winds in the tropical Pacific. In its positive phase, warmer waters enhance convection and rainfall across the Pacific, often preconditioning El Niño events. In its negative phase, cooler waters suppress	https://psl.noaa.gov/data/timeseries/month/data/pmm.data

		convection, leading to drier tropical conditions. The PMM influences the onset of ENSO events and plays a key role in shaping tropical and global climate variability, including rainfall over Africa.	
Pacific–North American Pattern	PNA	The PNA pattern is a major mode of atmospheric variability in the Northern Hemisphere, reflecting recurring pressure anomalies over the North Pacific and North America. The PNA index is based on standardized 500 hPa geopotential height anomalies at four specific locations. Its phases correlate with temperature and precipitation anomalies across North America. The PNA influences regional weather by modulating the strength and position of the East Asian jet stream, affecting storm tracks and climate patterns. Through atmospheric teleconnections, the PNA can also impact tropical circulations, with potential links to rainfall variability in the Sahel and parts of northern Africa.	https://psl.noaa.gov/data/correlation/pna.data
Quasi-Biennial Oscillation	QBO	The QBO is a regular oscillation of easterly and westerly winds in the tropical stratosphere, with a cycle of about 28–30 months. In its westerly phase, tropical cyclone activity increases, especially in the Pacific and Atlantic. In the easterly phase, cyclone formation weakens, and stratospheric ozone distribution shifts. The QBO modulates stratosphere–troposphere interactions and can influence tropical convection, potentially affecting rainfall variability in regions such as the Sahel and equatorial Africa.	https://psl.noaa.gov/data/correlation/qbo.data
Sahel Precipitation	Sahel P	Sahel Precipitation refers to the annual rainfall in Africa's Sahel region (south of the Sahara Desert) and is influenced by tropical Atlantic Sea surface temperatures and atmospheric circulation. Positive phases (increased rainfall) improve agriculture and water resources, while negative phases (drought) lead to famine and heightened socio-economic impacts.	https://psl.noaa.gov/data/correlation/sahelrain.data
Southern Oscillation Index	SOI	The SOI is calculated from the air pressure difference between Tahiti (central Pacific) and Darwin, Australia (western Pacific). Positive SOI values indicate La Niña conditions with high pressure over Tahiti and low pressure over Darwin, often linked to increased rainfall in the Sahel. Negative SOI values correspond to El Niño conditions, typically associated with drier Sahel conditions and shifts in global climate patterns.	https://psl.noaa.gov/data/correlation/soi.data
Solar Flux	-	Solar flux measures the amount of solar energy reaching Earth, reflecting solar activity cycles. Increased solar flux can lead to warming and changes in atmospheric circulation, which may influence rainfall patterns in Africa. Lower solar flux periods tend to coincide with cooler and more stable climate conditions, potentially affecting the Sahel rainfall variability indirectly.	https://psl.noaa.gov/data/correlation/solar.data
Tropical Northern Atlantic Index (TNA)	TNA	The TNA measures sea surface temperature anomalies in the tropical North Atlantic (5°N–25°N, 15°W–60°W). Positive phases with warmer SSTs are associated with increased rainfall along the West African coast and enhanced tropical cyclone activity. Negative phases correspond to cooler SSTs, reduced tropical rainfall, and weaker cyclone activity, often linked to drought conditions in the Sahel.	https://psl.noaa.gov/data/correlation/tna.data
Trans Nino Index	TNI	The TNI analyzes spatial shifts in El Niño and La Niña events by measuring SST differences between the eastern tropical Pacific (Niño-1+2) and central tropical Pacific (Niño-4). Positive TNI phases indicate eastward-shifted El Niño effects, increasing rainfall in the eastern Pacific and often suppressing rainfall in the Sahel. Negative phases reflect eastward shifted La Niña effects, which can enhance Sahel precipitation by influencing tropical atmospheric circulation.	https://psl.noaa.gov/data/correlation/tni.data
Tropical Southern Atlantic Index	TSA	The TSA measures SST anomalies in the tropical South Atlantic (0°–20°S, 10°E–30°W). Warmer SSTs in the positive phase lead to increased rainfall along eastern South America and shifts in the Atlantic Hadley circulation, which can influence West African monsoon intensity. Cooler SSTs during the negative phase are linked to drought and reduced convection, potentially weakening Sahel rainfall.	https://psl.noaa.gov/data/correlation/tsa.data
Tropical Western Hemisphere warm pool	WHWP	The WHWP covers the Caribbean, Gulf of Mexico, and eastern tropical Pacific where SSTs exceed 28°C. Positive phases are characterized by increased temperatures, leading to stronger tropical cyclone activity and enhanced rainfall in surrounding regions. Negative phases correspond to cooler SSTs and reduced storm intensity. WHWP variability affects Atlantic atmospheric circulation and can modulate rainfall in the Sahel and West Africa.	https://psl.noaa.gov/data/correlation/whwp.data

West Pacific Index	WPI	The WPI measures atmospheric pressure differences in the tropical and subtropical western Pacific. In its positive phase, a strong high-pressure system weakens Asian monsoons and tropical cyclone activity. The negative phase, dominated by low pressure, enhances Asian monsoon strength and storm activity. Changes in the WPI influence tropical climate dynamics and can indirectly affect the Sahel by modulating global atmospheric circulation patterns.	https://psl.noaa.gov/data/correlation/wp.data

- Include more explanation or citation on how SHAP values are computed and interpreted in the clustering context for readers unfamiliar with explainable AI techniques.

Thanks for the comment. In the revised version of the manuscript, the Methodological Section has been improved providing a more detailed explanation of the SHAP analysis:

However, this criterion does not allow for a clear assessment of the impact of each climatic index on the clustering process. To enhance the interpretability of clustering analyses in hydrological studies, particularly concerning drought patterns, this study integrates SHAP (values with RF models. This approach addresses the limitations of traditional clustering methods, which often lack explanatory power regarding the influence of individual climatic variables on cluster formation.

SHAP, grounded in cooperative game theory, assigns each feature an important value for a particular prediction, offering a unified measure of feature influence across the model. In this study, SHAP values are employed to interpret the output of an RF classifier trained to predict cluster assignments based on climatic indices (Lundberg and Lee 2017). The process involves:

- *Model Training: An RF classifier is trained using climatic indices as input features and the cluster labels (obtained from initial clustering analyses) as the target variable.*
- *SHAP Value Computation: Post-training, SHAP values are computed for each feature, quantifying the contribution of each climatic index to the model's prediction for each data point. This computation considers all possible combinations of features, ensuring a fair distribution of importance among them .*
- *Interpretation: The resulting SHAP values provide insights into how each climatic index influences the assignment of data points to specific clusters. Positive SHAP values indicate a feature's positive contribution to predicting a particular cluster, while negative values suggest a negative contribution.*

By employing this SHAP-driven approach, the study transforms clustering from a purely statistical exercise into an interpretable framework that reveals the underlying climatic drivers of drought patterns. This enhanced interpretability facilitates more informed decision-making and targeted adaptation strategies, especially in regions like the Sahel, where drought dynamics are influenced by complex interactions among multiple climatic factors.

This methodology aligns with recent advancements in explainable AI, where SHAP values have been utilized to enhance the interpretability of clustering analyses in various domains (Cohen et al. 2023). By integrating SHAP with RF models, the study not only identifies homogeneous drought regions but also elucidates the specific climatic variables driving these patterns, thereby contributing to more effective drought mitigation and resource management strategies.

Results

- Provide statistical significance or validation metrics for SHAP impacts (e.g., confidence intervals or feature importance rankings).

  Thanks for the comment. In supplementary material Table S5 has been reported, providing the SHAP Feature Importance Ranking with the Confidence Intervals. The text in the paper has been also updated accordingly. Below an extract of the updated text:

  In Cluster C1, the AMO, CAR and TNA emerged as the most influential variables, with mean absolute SHAP values of 0.088, 0.72 and 0.059, respectively (see Table S5). Their distributions are notably skewed toward positive SHAP values, with dense concentrations between 0.05 and 0.15. This pattern indicates a strong and consistent association between high index values and increased likelihood of C1 classification. Moderately influential indices such as WHWP, NTA, and AMM present narrower spreads (-0.05 to 0.2) and more symmetric profiles, suggesting subtler but still directional contributions. Conversely, indices like PDO, GMT, IPWP, and TSA show very limited SHAP influence, with values clustered near zero and minimal dispersion, highlighting their negligible role in defining this cluster.

  Cluster C2, in contrast, was characterized by AMO and the NTA indices as the most important features (mean absolute SHAP equal to 0.096 and 0.084, respectively), followed by CAR and TNA. These variables show significant spread on both sides of zero, implying a bidirectional influence where both high and low values can affect classification, depending on the context. Secondary contributors such as IPWP, AMM, and GMT exhibit tighter distributions centered around zero but with occasional asymmetries, pointing to context-dependent roles. Sahel P, PDO, and TSA remain minimally influential, with narrow SHAP ranges and modes at or near zero. Compared to Cluster C1, the SHAP profiles in C2 suggest greater interaction complexity among variables rather than dominance by a few.

  For Cluster C3, NTA dominated the feature importance ranking (mean absolute SHAP: 0.102), followed by AMO (0.080) and WHWP (0.072). These distributions are distinctly positively skewed, and the color gradient confirms that high feature values strongly align with positive SHAP contributions. Variables such as CAR, TNA, and IPWP *follow a similar, though slightly less pronounced, pattern. Mid-tier contributors like GMT, AMM, and TSA are more symmetrically distributed, with modal SHAP values just above zero. Finally, Sahel P and PDO again register as the least impactful, mirroring the behavior observed in the other clusters.*

Table S5. SHAP Feature Importance Ranking with Confidence Intervals. The color bar ranges from red (low values) to green (high values).

Classe	Feature	Mean Absolute SHAP values	Lower 95% Confidence Interval	Upper 95% Confidence Interval
C1	AMO	0.088	0.079	0.098
	CAR	0.072	0.064	0.081
	TNA	0.059	0.051	0.066
	WHWP	0.051	0.045	0.057
	NTA	0.042	0.038	0.048
	AMM	0.033	0.029	0.037
	Sahel P	0.013	0.011	0.014
	PDO	0.009	0.008	0.011
	GMT	0.006	0.005	0.006
	IPWP	0.002	0.002	0.002
	TSA	0.002	0.002	0.002
C2	AMO	0.096	0.091	0.101
	NTA	0.084	0.079	0.088
	CAR	0.077	0.072	0.081
	TNA	0.067	0.063	0.072
	WHWP	0.061	0.056	0.066
	IPWP	0.029	0.026	0.033
	AMM	0.027	0.025	0.030
	GMT	0.023	0.020	0.027
	Sahel P	0.014	0.013	0.016
	PDO	0.009	0.008	0.011
	TSA	0.007	0.006	0.008
C3	NTA	0.102	0.094	0.109
	AMO	0.080	0.073	0.087
	WHWP	0.072	0.067	0.078
	CAR	0.061	0.057	0.066
	TNA	0.059	0.055	0.064
	IPWP	0.030	0.027	0.033
	GMT	0.027	0.024	0.030
	AMM	0.012	0.011	0.014
	TSA	0.006	0.006	0.007
	Sahel P	0.004	0.003	0.004
	PDO	0.002	0.002	0.002

- The explanations of Beeswarm plots can be expanded for clarity.

Thanks for the comment. The explanation of Beeswarm plots has been improved as suggested by the Reviewer:

In the SHAP beeswarm plots (Figure 9), the x-axis represents SHAP values—the impact of each feature on the clustering outcome—while the color gradient (Feature value) encodes the actual correlation value between the climatic index and SPEI-12 for each data point, ranging from low (blue) to high (red). This dual encoding enables a nuanced interpretation of the model's behavior: the position along the x-axis reflects the strength and direction of influence, while the color reveals whether strong or weak correlations drive the effect.

- Include more information on model performance (e.g., accuracy, F1-score of RF classification for clusters).

Thanks for the comment. More details on model performance have been provided in the text:

To evaluate the relative influence of each climatic index on the clustering process and assess the predictive performance of the classifier, we employed an explainable AI approach that integrates a Random Forest (RF) classifier with SHAP. The RF model, a robust tree-based ensemble algorithm, effectively captures complex nonlinear interactions among variables but lacks inherent interpretability. To address both model performance and transparency, a comprehensive protocol was implemented.

First, the dataset was split using stratified sampling into training (90%) and testing (10%) subsets to preserve the original class distribution. A Random Forest classifier (100 estimators, criterion=Gini, random_state=42) was trained on the training data, and standard evaluation metrics—accuracy, class-wise precision, recall, F1-score, and the confusion matrix—were computed on the test set. The model achieved an accuracy of 0.985 on the independent test set. Class-wise precision, recall, and F1-scores were all above 0.97, confirming the classifier's strong discriminative power (see Table S4). Second, model explainability was addressed using SHAP values computed through the TreeExplainer framework. Beeswarm plots were generated for each cluster to visualize the magnitude and direction of feature contributions. Moreover, for each cluster, mean absolute SHAP values were computed for each feature, and a bootstrap procedure (n = 100) was performed to calculate 95% confidence intervals, providing statistical robustness to the importance rankings.

In addition, Table S4 has been provided in supplementary material, reporting the output accuracy of the Random Forest model.

Table S4. Output accuracy of the Random Forest model. The color bar ranges from red (low values) to green (high values).

Clusters	precision	recall	f1-score	support
C1	1	0.97	0.985	33
C2	0.964	1	0.982	54
C3	1	0.978	0.989	46
accuracy			0.985	133
macro average	0.988	0.983	0.985	133
weighted average	0.985	0.985	0.985	133
Overall Random Forest Accuracy	0.985			

Discussion

- Integrate more discussion on potential policy or adaptation strategies based on cluster-specific vulnerabilities.

  Thanks for the comment. In Section 4.3 "*Advancing Hydrological Clustering: From Conventional Methods to SHAP-Enhanced Insights*" details related to adaptation strategies based on the cluster outcomes are now reported:

  In addition, the spatial heterogeneity revealed across the three clusters highlights the need for targeted adaptation strategies that align with each cluster's specific climatic vulnerabilities. Cluster C2, which faces the most severe drought intensification, would benefit from proactive investment in water harvesting infrastructure, drought-resilient crop varieties, and transboundary water governance mechanisms to manage shared resources. Cluster C1, more strongly influenced by global warming indicators such as GMT and IPWP, may require policies focused on long-term resilience—such as promoting sustainable groundwater extraction, enhancing soil moisture retention through agroecological practices, and integrating climate-smart irrigation systems. In contrast, Cluster C3, where local and regional dynamics dominate, presents an opportunity for community-based water management, improved land use planning, and localized climate services tailored to support decision-making at the grassroots level. These differentiated strategies are crucial to building adaptive capacity in the Sahel and ensuring that resource allocation reflects both scientific insight and regional socio-environmental contexts.

- Acknowledge limitations such as the temporal range of the data (1951–2018), and possible bias due to data resolution or missing climatic drivers.

  Thanks for the comment. In Section 4.4 "*Limitations and Future Directions*" details related to possible bias due to data resolution or missing climatic drivers are now reported:

  Furthermore, the temporal range of the analysis (1951–2018), although selected to ensure consistency and adequate overlap among multiple climate indices, may not fully capture recent accelerations in climate change and extreme event frequency, especially post-2018. As newer datasets become available, extending the analysis to include the most recent years will be critical for capturing ongoing hydroclimatic shifts. Moreover, while the 0.5° spatial resolution of the Global SPEI Database is adequate for regional-scale assessments, it may smooth out local variations critical for decision-making at finer administrative levels. This can introduce spatial biases, particularly in areas where terrain, land use, or rainfall gradients are highly variable. Finally, despite the broad suite of 31 climate indices considered, the exclusion of potentially relevant drivers—such as dust aerosol concentrations, local vegetation indices, or land surface temperature—could limit the full explanatory power of *the model. Incorporating such variables in future iterations may improve the detection of drought triggers and feedbacks, especially where local biogeophysical processes play a pivotal role.*

Figures and Tables

- Improve color consistency and legends for clarity (e.g., avoid ambiguous shades).
- Add numerical cluster centroids or representative climate patterns for each cluster.

Different figures have been revised to avoid ambiguous shades:

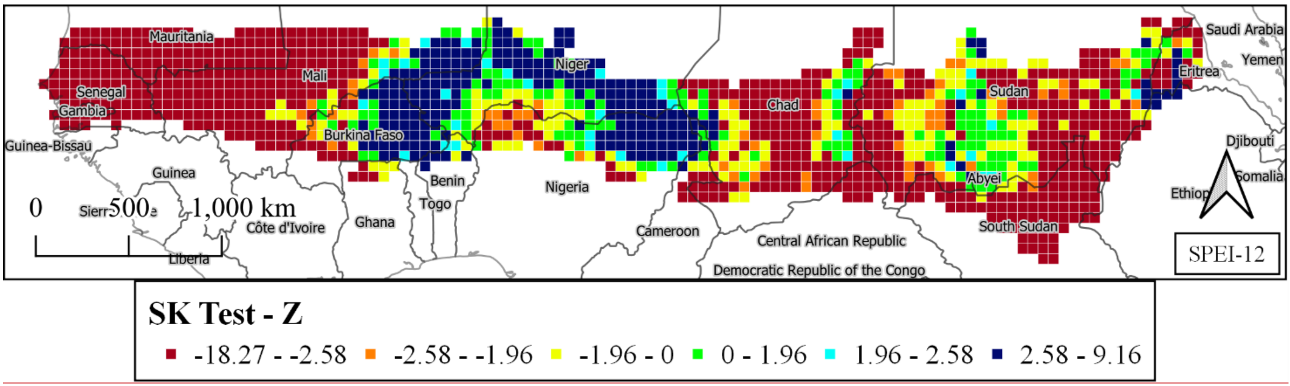

Figure 3: Z parameter of the SK test: SPEI-12 map (a)

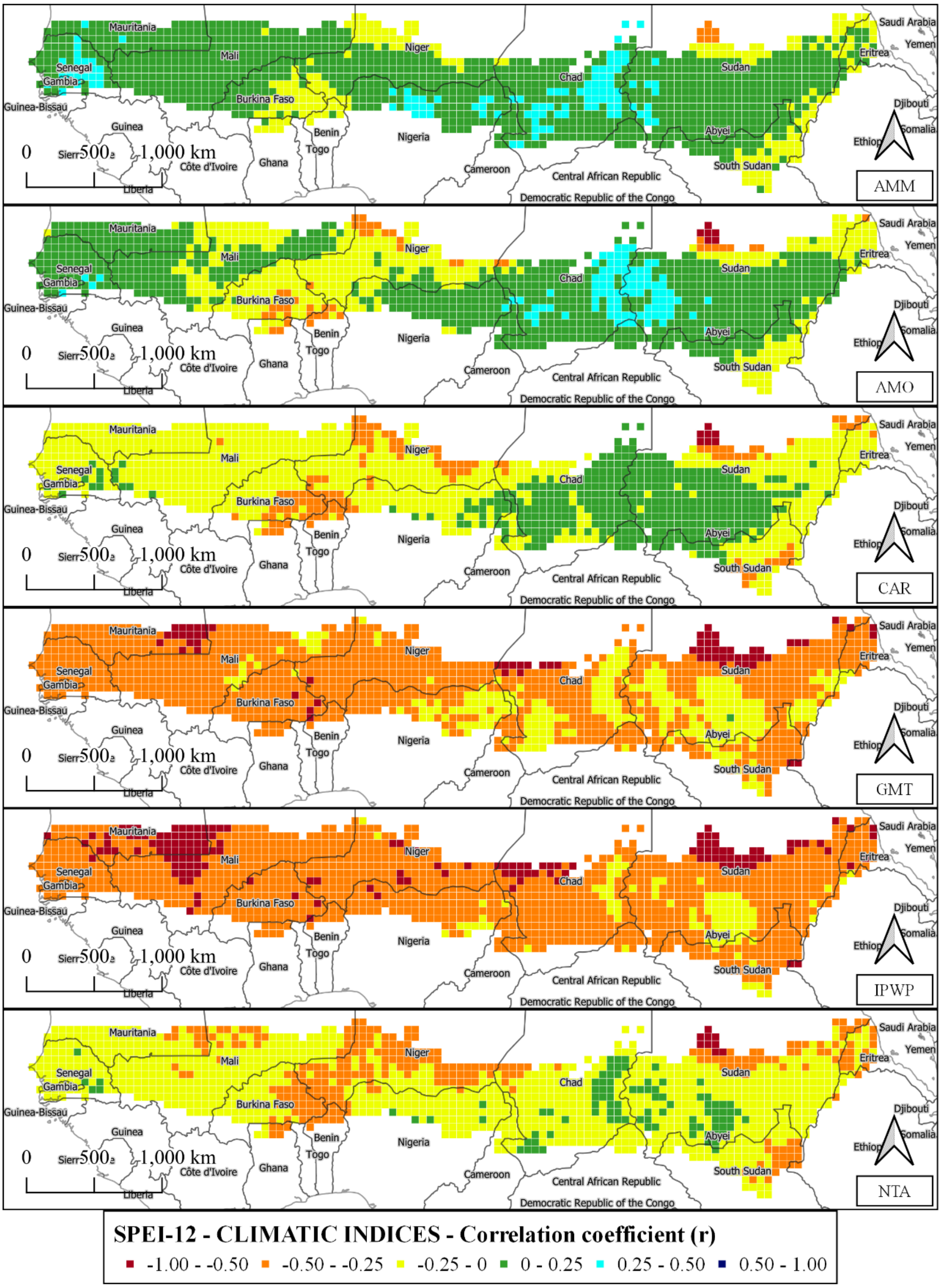
Mauritania
Mali
Niger
Chad
Sudan
Saudi Arabia
Yemen
Eritrea
Senegal
Gambia
Guinea-Bissau
Burkina Faso
Guinea
Benin
Togo
Nigeria
Ghana
Côte d'Ivoire
Liberia
Cameroon
Central African Republic
Democratic Republic of the Congo
Abyei
South Sudan
Djibouti
Somalia
Ethiop
Sierr
0 500 1,000 km
AMM
AMO
CAR
GMT
IPWP
NTA
SPEI-12 - CLIMATIC INDICES - Correlation coefficient (r)
-1.00 - -0.50
-0.50 - -0.25
-0.25 - 0
0 - 0.25
0.25 - 0.50
0.50 - 1.00

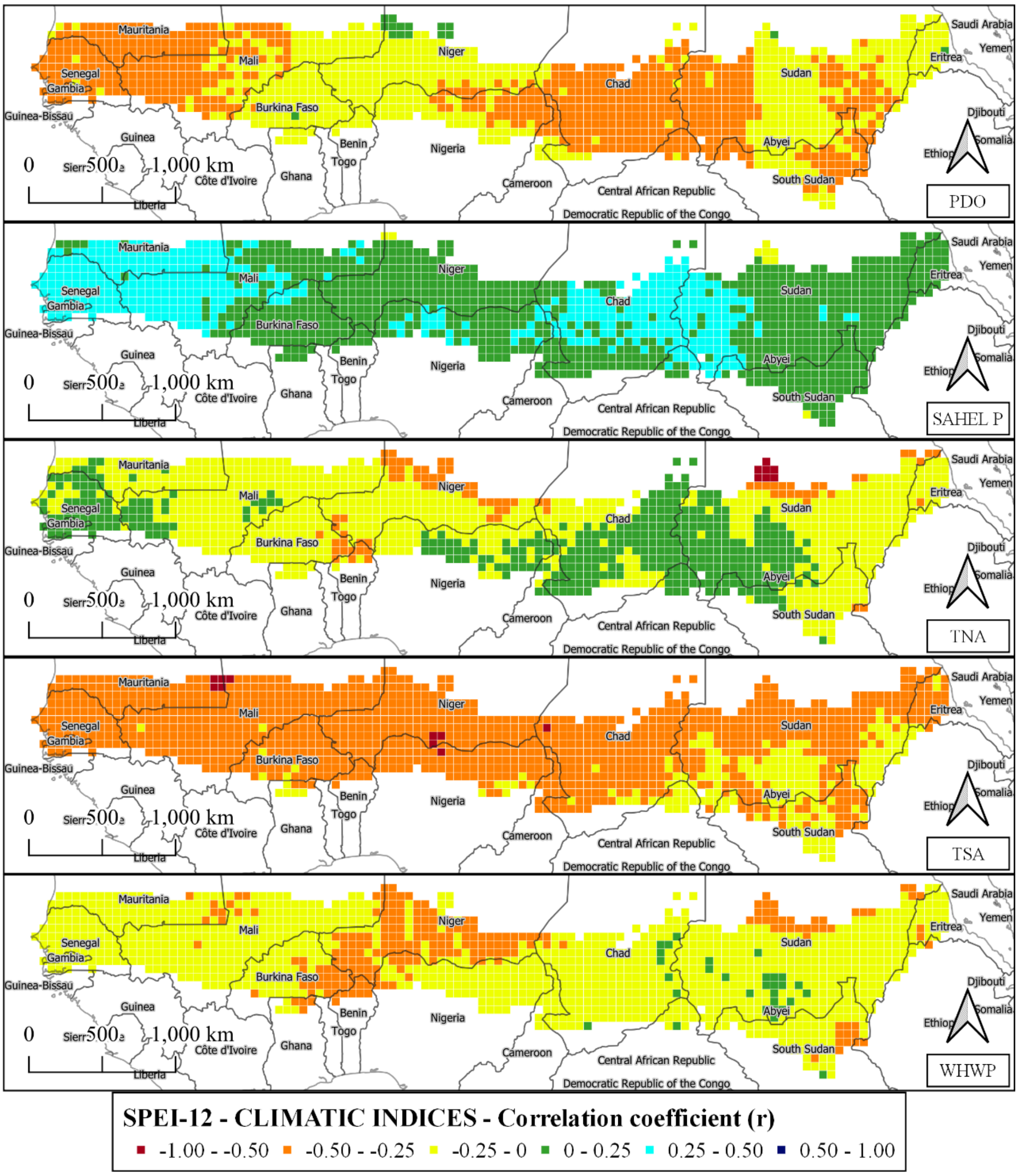

Figure 5. Maps of the correlations between SPEI-12 gridded data and the most correlated climatic indices (continue).

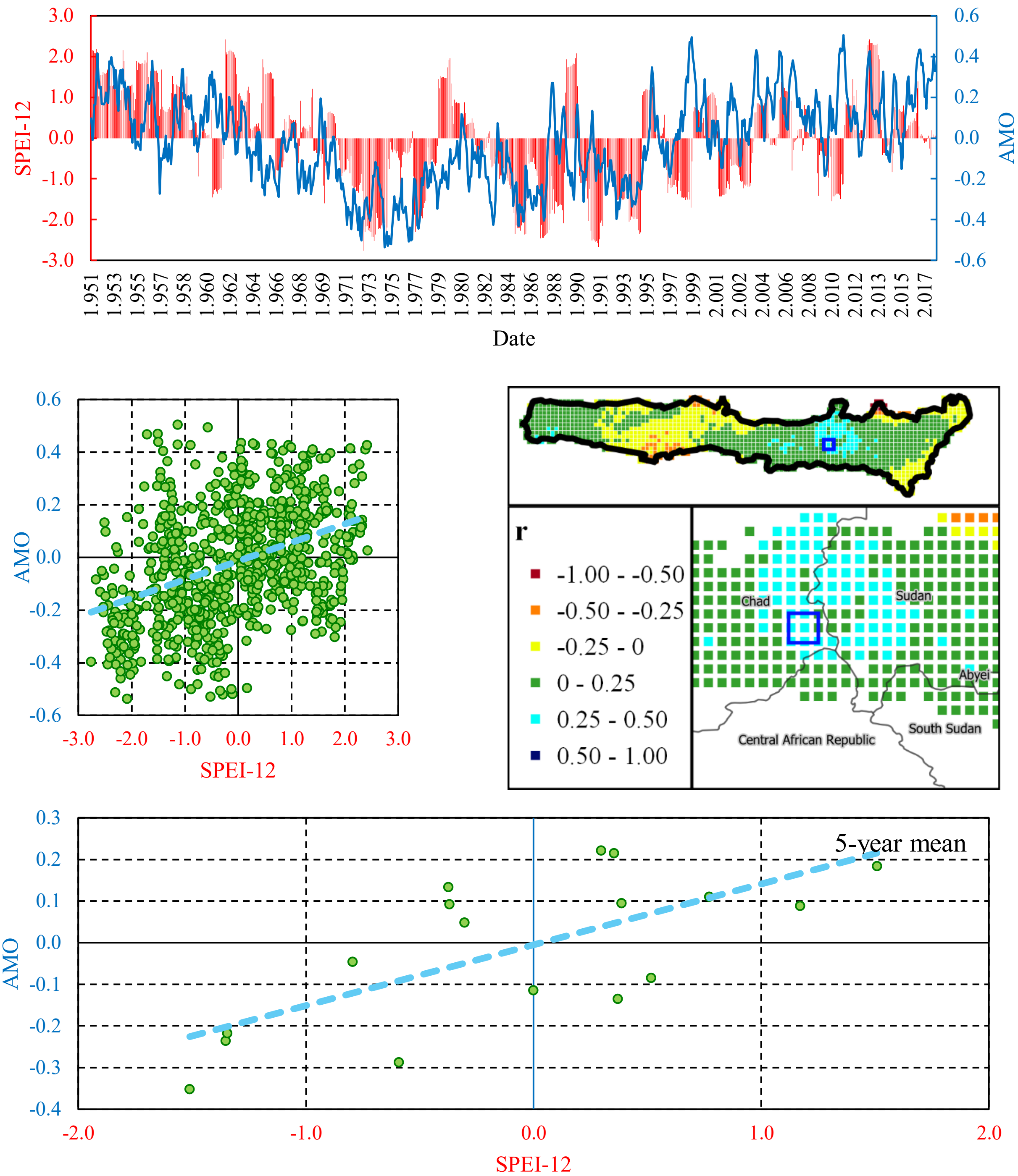

Figure 6. Correlation analysis between SPEI-12 for Cell 2042 and AMO. The figure presents the time series of AMO and SPEI-12 for Cell 2042, located at the border between Chad and Sudan. Additionally, it includes a scatter plot illustrating their relationship on both a monthly scale and a five-year mean scale.

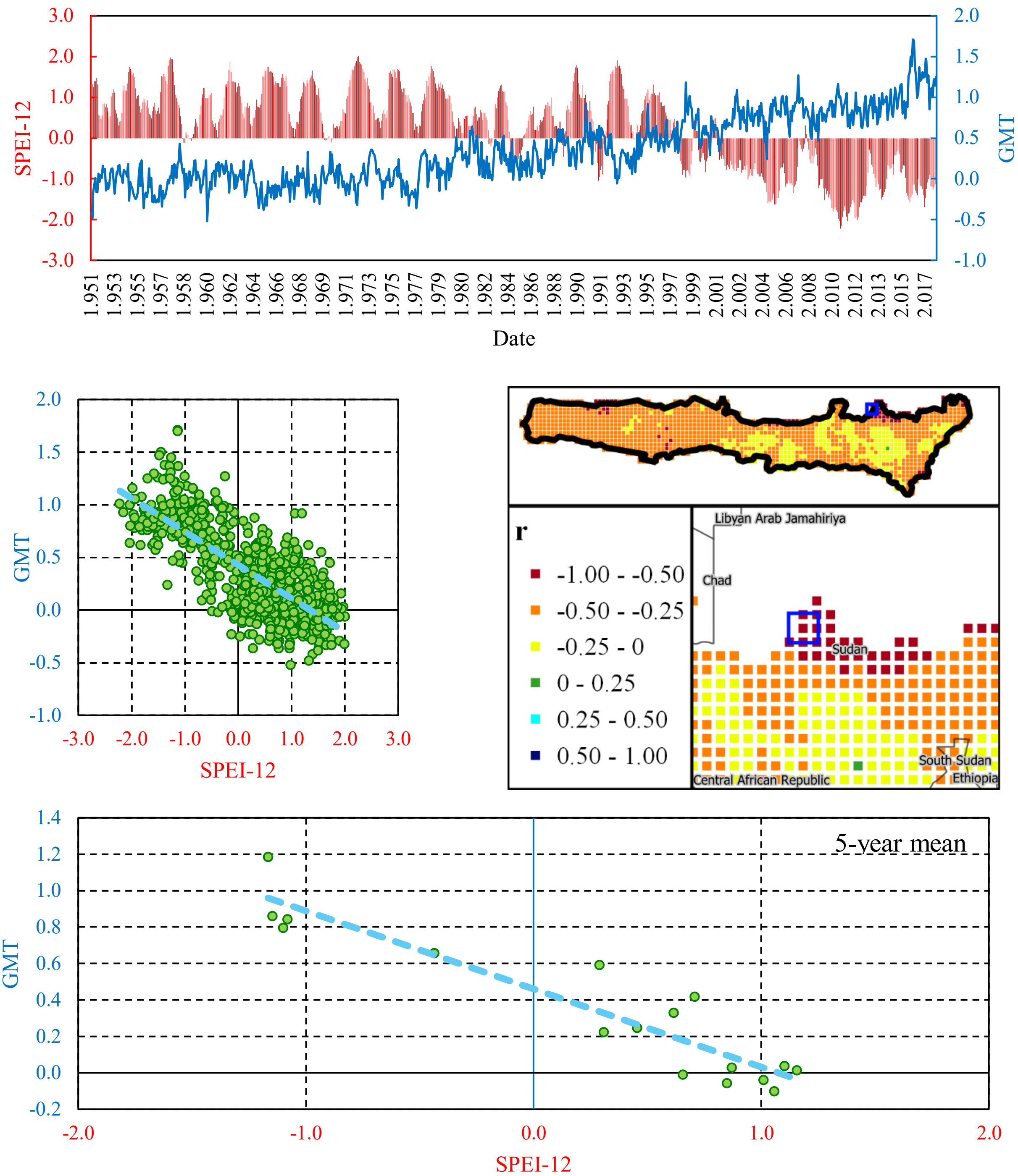

Figure 7. Correlation analysis between SPEI-12 for Cell 2319 and GMT. The figure presents the time series of AMO and SPEI-12 for Cell 2319, located at the Sahel's border in Central Sudan. Additionally, it includes a scatter plot illustrating their relationship on both a monthly scale and a five-year mean scale.

Language and Style

- Consider simplifying overly dense or jargon-heavy sentences (especially in the Introduction and Discussion).
- Check for consistency in the use of abbreviations (e.g., GMT vs. Global Mean Temperature) and ensure all acronyms are introduced properly.

Thanks for the comment. We have carefully revised the text, particularly in the *Introduction* and *Discussion* sections, to simplify overly dense or jargon-heavy sentences and improve overall readability. Additionally, we reviewed all abbreviations and acronyms throughout the manuscript to ensure consistent usage and that each term is properly introduced at first mention). These changes have been implemented to enhance both clarity and accessibility for a broader audience.

Novelty and Impact

- Emphasize more clearly in the Conclusion how the framework can be generalized to other regions beyond the Sahel.

We thank the Reviewer for this insightful suggestion. In response, we have revised the Conclusion section to more clearly emphasize the generalizability of our proposed framework. Specifically, we now highlight that the modular structure—comprising seasonal trend analysis, cross-correlation with large-scale climate drivers, and explainable machine learning via SHAP-driven clustering—can be readily adapted to diverse hydroclimatic contexts beyond the Sahel. This includes temperate, monsoonal, and arid regions where drought dynamics are governed by both local conditions and global climate teleconnections. The revised text underscores the framework's flexibility, interpretability, and potential to support data-informed drought risk assessment and adaptation strategies across geographically and climatically varied settings:

This study presents a comprehensive framework for assessing drought variability in the Sahel by integrating trend analysis, cross-correlation, and an innovative SHAP-driven clustering approach. The analysis revealed that 57.5% of the region exhibits a significant drying trend in SPEI-12, particularly in the western and southeastern Sahel, driven by increasing temperatures and declining precipitation. Conversely, 19.3% of the region shows statistically significant wetting trends, highlighting the spatial heterogeneity of drought evolution primarily through increased evapotranspiration and reduced soil moisture availability. At a regional scale, AMO and NTA emerged as key modulators of drought variability, influencing distinct drought-prone zones. Clustering identified three major drought regimes, with Cluster C2 (western Sahel: Senegal, Mauritania, Mali) experiencing the most severe intensification (Z = -5.04).

The SHAP-driven clustering approach integrates a Random Forest (RF) model with SHAP values to identify distinct drought patterns across the Sahel. By quantifying the contribution of each climatic index to the clustering results, this method makes the model's decision-making process transparent and highlights the prominent influence of AMO and NTA on regional drought variability. This level of interpretability allows for a deeper understanding of the climatic mechanisms behind spatial drought patterns, offering a robust basis for designing targeted adaptation strategies.

Beyond its application in the Sahel, the proposed framework offers strong potential for generalization to other drought-prone regions worldwide. Its modular structure—combining seasonal trend detection, teleconnection analysis, and *explainable machine learning—can be readily adapted to different hydroclimatic contexts, including temperate zones, monsoonal climates, and arid environments. By incorporating local drought indices and relevant climate drivers, this methodology can support region-specific assessments while maintaining the advantages of transparency and model interpretability. As such, it provides a scalable and transferrable tool for advancing drought risk management in a changing global climate.*

By bridging advanced statistical analysis with explainable AI techniques, this study contributes a novel and interpretable approach for understanding climate impacts on regional water security, offering actionable insights for policymakers, researchers, and resource managers well beyond the Sahel context.